IJME

*Int. J. of Applied Mechanics and Engineering, 2023, vol.28, No.1, pp.84-94*
DOI: 10.59441/ijame-2023-0008

# EFFECT OF SOIL CONSOLIDATION ON THE FRACTALITY OF THE FILTRATION LAW

Geylani PANAHOV* and Parviz MUSEIBLI
Department of Fluid Mechanics, Institute of Mathematic and Mechanics
Azerbaijan National Academy of Sciences, B. Vagabzadeh St., 9, AZ1141, Baku, AZERBAIJAN
E-mail: geylani.panahov@imm.az

Babek SULTANOV
Baku State University, Theoretical and Continuum Mechanics Department
Akademik Zahid Xalilov st., 33, AZ1148, Baku, AZERBAIJAN

In this paper, the effect of consolidation of the soil structure on the fractality of the fluid flow was evaluated. The equation of fractal law of flow in the porous medium under consolidation of two-phase, fully fluid-saturated soil was determined. Given all the simplifications, as well as the undoubted importance of the nature of the porous medium, which primarily determine the possible processes of both consolidation and fractal flow based on the results of the studies, we can conclude that a homogeneous porous reservoir at given parameters under the effect of groundwater pressure will expand its fractal structure.

**Keywords:** soil; consolidation, fractals, filtration law, flow, porosity, rheology.

## 1. Introduction

The theory of consolidation of fluid-saturated layers considers the process of soil particles bringing them closer together and reducing the pore volume. Related to fluid displacement from pores, this theory is attracting increasing attention due to the increasing volume of underground recovery in tight and high-pressure reservoirs. Being a problem of non-stationary flow in a deformable medium, and taking into account the variable porosity and permeability of the ground, its multiphase nature and the complex rheology of the phase components, it is sometimes not analytically solvable. In this case, appropriate numerical methods are used to analyze the situation by [1, 2].

The soil pressure transmitted to fluid-saturated soil is distributed between the fluid contained in the pores and the soil skeleton, i.e., the mineral particles encircled by the fluid film and bonded together to form a single framework. The stress in the soil skeleton causes it to compress visibly and affects the shear resistance of the soil [3].

The excess pressure in the pore fluid is called the neutral pressure and is denoted by $P$. If the neutral pressure is positive, it is called the pore fluid pressure according to Terzaghi [4]. For an incompletely fluid-saturated soil according to Bishop we have from Mashchenko *et al.* [5]:

$$\sigma_z^{'} = \sigma_z - \left[ p_f + (1-c)\left( p_a - p_f \right) \right] \tag{1.1}$$

where $p_f$ is the pressure in the pore fluid; $p_a$ is the pressure in the soil pores; $c$ is an experimentally determined coefficient.

* To whom correspondence should be addressed

At full fluid saturation $c = 1$ and Eq.(1.1) turns into dependence:

$$\sigma_z = \sigma_z^{'} + p = const.$$

For a complex stress state, this dependence has the form:

$$p_a\, T = T_{\sigma'} + T_p$$

where $T_{\sigma'}$ is the effective stress tensor; $T_n$ is the neutral stress tensor. The $T_{\sigma'}$ tensor, in turn, can be decomposed into a globular tensor of effective stresses $T_{\sigma'}^{0}$, which causes volume deformation of the porous skeleton, and a deviator of effective stresses $D_{\sigma'}$, which causes shear deformation:

$$T = T_{\sigma'}{}^{0} + D_{\sigma'}\,.$$

The neutral stress tensor $T_n$ creates only a pressure in the pore fluid without causing shear, i.e., it is a ball tensor:

$$T_n = T_n{}^{0}\,.$$

Volumetric deformations of the soil skeleton develop in time due to the viscous resistance of the inter-particle bonds. Since such deformations are not related to the extrusion of free pore fluid, they are most commonly found in highly compacted soils in which the liquid phase is a cohesive fluid. In tests of highly compacted clays, in which the fluid is in a bound state, all volumetric deformation can be regarded as volumetric creep. For normally compacted soils, and even less compacted ones, volumetric deformations are caused both by creep of the soil skeleton and by moisture filtration.

The flow process mainly occurs during the initial testing period, while the soil skeleton creep - observed later on when most of the moisture has been displaced, a sign of which is the dissipation of the pore pressure and its drop to zero.

The volumetric creep equations have the form [6]:

$$\varepsilon_m = f^*\left(\sigma_m^{'}\right)\Phi^*(t)$$

where $f^*\left(\sigma_m^{'}\right)$ is a function characterizing the relationship between the average normal effective stress $\sigma_m^{'}$ and the average linear strain $\sigma_m$; $f^*\left(\sigma_m^{'}\right)$ is a function of volume creep.

A combined analysis of the equation of filtration consolidation and the equation of creep of the soil skeleton will make it possible to solve the problem of linear compaction of the soil, taking into account primary and secondary consolidation. It is possible to take into account compressibility of the pore fluid as well as mineral particles themselves, presence of initial hydraulic head gradient, influence of structural strength and material aging, variability of filtration coefficient, etc. To consider secondary consolidation of the soil in the mechanical model, viscous, Newtonian elements are introduced into this model in addition to the flow elements, which are connected to the elastic elements modeling the soil skeleton. As a result, the skeleton is provided not only with elastic but also with viscous properties. Such a model is a combination of the model and additional viscous elements [5, 6].

All the elastic elements, each representing a Kelvin-Voigt model, are connected to one another in series to form a combined model. This model describes the soil skeleton. Assuming that the parameters of all

repeating elements of the model are the same, corresponding to a depth-homogeneous soil layer, the soil skeleton deformation equation would be of the form [2].

$$\varepsilon = a_0^{'}\left[\sigma'(t) + \int_0^t \sigma'(\nu) K(t-\nu)\, d\nu\right]$$

where $\sigma'(t)$ is the time-varying effective pressure, and $K(t-\nu) = \bar{a}_0 e^{-\frac{1}{T_p}(t-\nu)}$, where $\bar{a} = \left(a_0^{''} - a_0^{'}\right) / \left(a_0^{'} T_p\right)$, $a'$ and $a''$ - instant (under $t = 0$) and finite (under $t = \infty$) values of the coefficient of relative compressibility; $T_p$ - post-action time.

The model considering the pore fluid consists of filtration elements and elastic elements connected to them according to the Maxwell-type model with the compressibility factor $a_f$, modeling the compressibility of the pore fluid. A dry friction element is connected to the piston rod, which simulates the initial pore pressure $p_0$ that causes the initial head gradient. The fluid can begin to shift only when the pressure in the pore fluid exceeds the value of $p_0$. Considering displacements of model points and making differential equilibrium condition, it is possible to obtain the equation of deformation [5]:

$$\frac{\partial e}{\partial t} + a_f e_{cp} \frac{\partial p}{\partial t} = \frac{1 + e_{cp}}{\gamma_f} K_f \left( \frac{\partial^2}{\partial x^2}(p - p_0) + \frac{\partial^2}{\partial z^2}(p - p_0) \right) \tag{1.2}$$

where $K_f$ is the pore fluid filtration coefficient, cm/h; $e$ and $e_a$ are time and average values of the porosity coefficient; $t$ is time; $a_f$ is the fluid compressibility coefficient; $\gamma_f$ is the fluid density; $p$ is the pore pressure; $p_0$ is the initial pore pressure.

Substituting Eq.(1.2) into Eq.(1.1) (under $\varepsilon = \Delta e$), we obtain a pattern of soil compaction taking into account primary and secondary consolidation, compressibility of the liquid phase and the presence of initial pore pressure.

Using multielement models, in contrast to conventional models, it is possible to obtain the equation of deformation of the soil skeleton in the integral form corresponding to the theory of hereditary creep [5].

The creep phenomenon is related to a property of the soil body such as its strength, leading to consolidation of the soil. The ground creep development causes a progressive flow of pore fluid. Thus, during prolonged loading, the soil is subjected to stresses that may be less than the value of the strength under load.

The results of experimental research on the influence of soil deformation on fluid filtration parameters show that as a result of soil deformation, soil permeability and pore volumes of the sample occupied by the fluid decrease [7, 8].

In the process of development of hydrocarbon fields with time the effective pressure increases, therefore, unsteadily decreases the volume of pore space, which leads to a significant decrease in the porosity coefficient. The change of porosity coefficient and pore volume of the fluid saturated sample, directly affects the rate of pressure drop by [7, 8].

We determine a rock element large enough to neglect the effect of skeletal and pore space heterogeneity. For such a rock, a differential equation for the reservoir porosity factor change is obtained in general form:

$$\frac{dk_n}{k_n} = \left(\beta_{sk} - \beta_{por}\right) d(\sigma - p) + \left(1 - \mu_p\right) \beta_{solid}\, dp - \left(1 - \mu_T\right) \alpha_T\, dT\ ,$$

here $\frac{dk_n}{k_n}$ is the change in the porosity coefficient, $\mu_p$ is the coefficient taking into account changes in the reservoir pore volume as a result of deformation of clay particles with changes in reservoir pressure, $\mu_t$ is the coefficient taking into account changes in the reservoir pore volume due to thermal expansion or contraction of clay particles with temperature changes. Thus, in the general case, the change in the reservoir porosity ratio depends on the effective stress $\sigma - p$, reservoir pressure $p$, temperature $T$, elastic and thermal properties of the soil skeleton reflected in the coefficients $\beta_{sk}, \beta_{por}, \beta_{solid}, \alpha_T$, as well as on the relative clay content of reservoirs $\eta_{cl}$ and other inclusions, elastic and thermal properties of clay minerals. This is a complex dependence and the solution of which in general form is associated with significant difficulties, not only mathematically, but mainly due to the complex nature of the change of elastic and thermal constants, depending on the lithological and petrographic composition of the soil, stresses, temperature. For pure unclayed sand or carbonate reservoirs, the change in the porosity ratio can be said to depend only on the amount of effective stress and elastic properties of the reservoir. And thus, we can say that it does not depend on changes in the reservoir pressure and temperature

$$\frac{dk_n}{k_n} \approx \left(\beta_{sk} - \beta_{por}\right) d\left(\sigma - p\right).$$

More compacted sedimentary soils, such as sandstones, siltstones, mudstones, Permian-Triassic soils from depths of $3000 - 4000\,m$ slightly less reduce their porosity under the action of isothermal compression, which seems to be explained by the high compaction of these soils. The lowest values of the porosity coefficient under isothermal compression are characterized by well-sorted sandstones and highly compacted argillites. The average decrease in porosity of these soils at the corresponding bedding depth of about $11{,}000\,m$ is just over $6\%$. For poorly sorted and poorly rounded sandstones, the same value is nearly $20\%$. In carbonate soils, there are very wide limits, changes in the porosity coefficient with changes in effective stresses. The most significant decrease in porosity up to $20\%$ was observed for low porous fine and hidden-crystalline limestones.

The smallest, about $2\%$, at the same stresses, for more porous dolomitized limestones. Such large changes in porosity in low-porous soils are probably due to the micro-cracks involved. Changes in the porosity coefficient reaching $40\%$ were observed by L.M. Marmorstein in the study of sandstones with basal and basal-porous type of cement. Such porosity changes are unusual for cemented sandy-clayey soils under elastic deformation. They may, for example, be related to irreversible phenomena in soils with little mechanical strength when the effective stress during loading exceeds the maximum effective stress at which the soils were at depth [9].

In particular, for example, the analysis of recent experimental results for samples from well sorted low clay medium-fine-grained quartz sandstones (quartz content in samples fluctuates within $84...95\ \%$), shows that the maximum permeability of the studied sample decreases at effective pressure value of $37\,MPa$, the permeability coefficient has decreased by $50{,}7\ \%$. And the character of dependence of relative permeability decrease of the sample on effective pressure growth has the character of inverse proportional dependence [10]. As a result, we obtain the fractal structure of fluid flow in soil with creep properties [11]. Recent studies also suggest the fractal nature of the filtration structure of the soil [12-14].

The construction of regularities of the effect of soils consolidation on the structure fractality is an urgent task. However, it is natural that the obtained generalized system of equations will be many times more mathematically complex, both in the sense of its solution and analysis. Therefore, the use of simplifying transformations and application of relatively simple numerical methods is preferable [15, 16]. If we assume in Eq.(1.2) that the fluid is practically incompressible ( $a_w = 0$, $\gamma_f = const$ ), and express the head function in the

form $H = \frac{p}{\gamma_f} + x$, where $x$ - is the height to a point above the comparison plane and describe the fractality in the form [17-21] we get

$$\left(D_{a_+}^{\alpha} H\right)(x) = \frac{1}{\Gamma(1-\alpha)} \frac{\partial}{\partial x} \int_a^x \frac{H(\xi)\, d\xi}{(x-\xi)^a},$$

$$\left(D_{a_+}^{\beta} H\right)(z) = \frac{1}{\Gamma(1-\beta)} \frac{\partial}{\partial z} \int_a^z \frac{H(\xi)\, d\xi}{(z-\xi)^a} \tag{1.3}$$

where Γ(1-α) is the Euler gamma-function, α is the fractality parameter of the filtration component, ξ is the length of fractal element, then it is possible to write Eq.(1.2) in the form:

$$\frac{\partial e}{\partial t} = (1+e)\left[\frac{\partial}{\partial x} k_x \left(\frac{\partial}{\partial x}\left(D_{a_+}^{\alpha} H\right)(x) - i_0\right) + \frac{\partial}{\partial z} k_z \left(\frac{\partial}{\partial z}\left(D_{0_+}^{\beta} H\right)(z) - i_0\right)\right]. \tag{1.4}$$

Here $i_0$ is the initial head gradient.

## 2. Problem formulation and solution methods

Consider the consolidation equation with regard to fractality in the following form:

$$\frac{\partial H}{\partial t} = C_v \left(\frac{\partial^2}{\partial x^2}\left(D_{a_+}^{\alpha} H\right)(x) + \frac{\partial^2}{\partial z^2}\left(D_{0_+}^{\beta} H\right)(z)\right). \tag{2.1}$$

Here, for simplicity, we assumed the absence of an initial head gradient $i_0$ and constancy and uniformity of filtration coefficients in different directions, $k_x = k_z = k = const$.

And also, here we assume a linear dependence of the porosity coefficient on stress, i.e.: $e = -a\sigma + b$, where $a$, $b$ are experimentally determined constants.

Hence

$$-\frac{\partial e}{\partial t} = \frac{\partial \sigma}{\partial t} = -2\frac{\partial p}{\partial t} = -2\gamma \frac{\partial H}{\partial t}.$$

Let us represent the ground as undisturbed, isotropic and homogeneous.

Thus, we need to find functions $H(t,x,z), C_v$ satisfying Eq.(2.1) in rectangle $Q$, and for $H(t,x,z)$ the conditions are

$$H(0,x,z) = H_0(x,z), \quad 0 < x < 1, \quad 0 < z < 1, \tag{2.2}$$

$$H(t,0,0) = \mu_0(t), \quad H(t,1,1) = \mu_1(t), \quad 0 < t < T, \tag{2.3}$$

$$H(T,x,z) = H_1(x,z), \quad 0 < x < 1, \quad 0 < z < 1. \tag{2.4}$$

Condition (2.3) is the final redefinition condition, i.e., the unknown is the coefficient $C_\nu$. To determine $C_\nu$ we obtain an inverse problem.

The function $C_\nu$ has to be defined simultaneously with the solution $H(t,x,z)$ of problems (2.1), (2.2)-(2.4). Problems (2.1), (2.2)-(2.4) are reduced to an auxiliary direct problem. For this purpose, we take $t=T$ in Eq.(2.1).
Then, using condition (2.4), we obtain

$$C_\nu = \frac{\dfrac{\partial H(T,x,z)}{\partial t}}{\dfrac{\partial^2}{\partial x^2}\left(D_{a_+}^{\alpha} H\right)(T,x) + \dfrac{\partial^2}{\partial z^2}\left(D_{0_+}^{\beta} H\right)(T,z)}. \tag{2.5}$$

Let us note that the denominator of expression (2.4) does not return to zero by virtue of the condition on $H(t,x,z)$. Thus, the function $H(t,x,z)$ satisfies the equation

$$\frac{\partial H}{\partial t} = \frac{\dfrac{\partial H(T,x,z)}{\partial t}}{\dfrac{\partial^2}{\partial x^2}\left(D_{a_+}^{\alpha} H\right)(T,x) + \dfrac{\partial^2}{\partial z^2}\left(D_{0_+}^{\beta} H\right)(T,z)}\left(\frac{\partial^2}{\partial x^2}\left(D_{a_+}^{\alpha} H\right)(x) + \frac{\partial^2}{\partial z^2}\left(D_{0_+}^{\beta} H\right)(z)\right). \tag{2.6}$$

The classical solvability of problems (2.5), (2.1)-(2.2) can be obtained, for example, by the method of weak approximation or by applying finite differences [22].

## 3. Numerical results

Consider the one-dimensional case on the coordinate $x$. We write the partial derivatives with the corresponding differences:

$$\frac{\partial H}{\partial t} \approx \frac{H_{i,k+1} - H_{i,k}}{\Delta t},$$

$$\frac{\partial^2}{\partial x^2}\left(D_{a_+}^{\alpha} H\right) = \frac{1}{\Gamma(1-\beta)}\frac{\partial^3}{\partial x^3}\int_0^x \frac{H(\xi,t)}{(x-\xi)^{\beta}} d\xi \approx$$

$$\approx \frac{1}{\Gamma(1-\beta)}\left(f_{i+1,k} - 3 f_{i,k} + 3 f_{i-1,k} - f_{i-2,k}\right)\left(\frac{1}{\Delta x}\right)^3$$

where:

$$f(x,t) = \int_0^x \frac{H(\xi,t)}{(x-\xi)^{\beta}} d\xi \approx f_{i,k} = \sum_{j=0}^{i-1} \frac{H_{j,k}}{(i-j)^{\beta}} \Delta x$$ - the left rectangle formula.

The initial and boundary conditions, as well as the corresponding parameters are presented in the following form:

$k=0$ and $0 \le i \le n$; $\quad H_{i,k} = H_0 = 1$,

$k \ne 0$ and $i=0$ or $i=n$; $\quad H_{i,k} = 0$,

$\beta = 0.5$ (fractality of the filtration law),

$\Gamma(1-\beta) \approx 1{,}77245$ ,

$\Delta t = 0.01$ , $\Delta x = 0.1$ , $k_{max} = m = 20$ , $i_{max} = n = 10$ .

Then expression (2.6) is rewritten as:

$$\frac{\partial H}{\partial t} = \frac{\dfrac{\partial H(T,x)}{\partial t}}{\dfrac{\partial^2}{\partial x^2}\left(D_{a_+}^{\alpha} H\right)(T,x)} \left( \frac{\partial^2}{\partial x^2}\left(D_{a_+}^{\alpha} H\right)(x) \right), \tag{3.1}$$

which in finite differences is rewritten as:

$$H_{i,k+1} = H_{i,k} + \frac{(H_{i,m} - H_{i,m-1})\left( f_{i+1,k} - 3 f_{i,k} + 3 f_{i-1,k} - f_{i-2,k} \right)}{\left( f_{i+1,m-1} - 3 f_{i,m-1} + 3 f_{i-1,m-1} - f_{i-2,m-1} \right)} .$$

Numerically solving this equation (3.1) we obtain the following graphs of fractality changes under this law of soil consolidation (Fig.1-4).

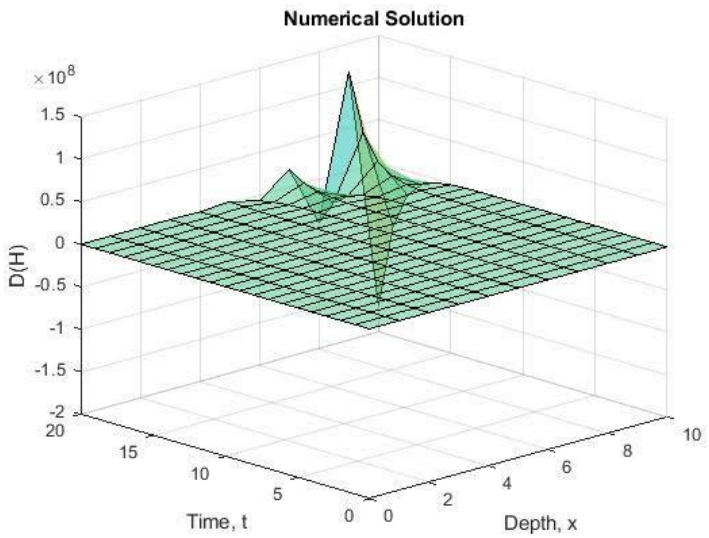


Fig.1. 3D graph of pressure function dependence on time and depth of layer.

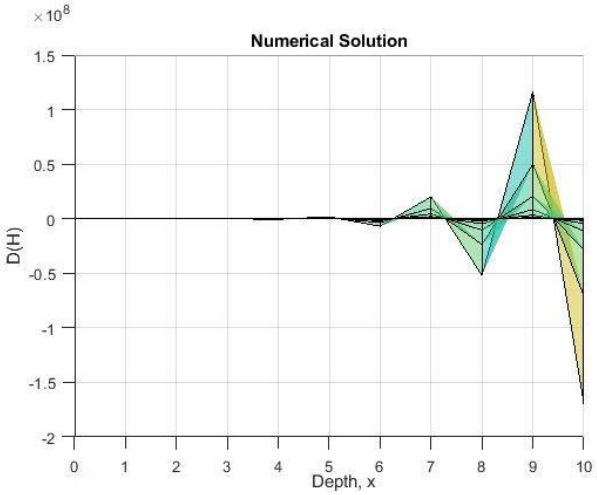


Fig.2. Dependence of pressure function on depth of layer.

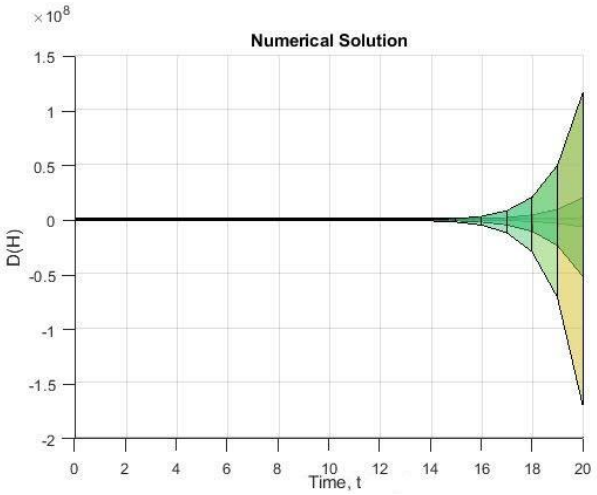


Fig.3. Dependence of pressure function on time.

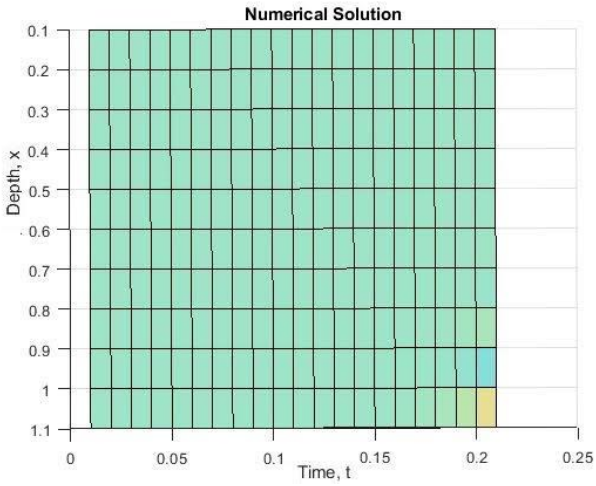


Fig.4. Fractality change by depth of layer and in time for a given consolidation law.

At the same time, the graph of the change in the consolidation coefficient $C_v$ is obtained as:

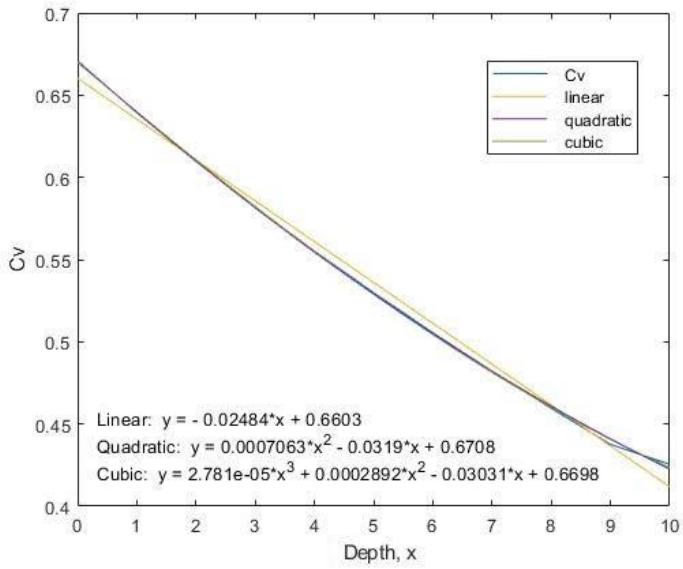


Fig.5. Changing the consolidation coefficient $C_v$ along the $x$-coordinate.

## 4. Conclusions

The following conclusions can be made from the research carried out:

1. The geo-mechanical behavior of soils results from the consideration of elastic, plastic and viscous properties depending on soil characteristics and conditions (shear rate and shear stress values) as well as the time scale of the measurement. Fractal models can be a tool for analyzing these phenomena, which depend on the time required to rearrange the soil's natural structure.
2. Under given initial and boundary conditions, as well as consolidation law, fractality change has practically increasing wave-like character with depth increase. There is also a sharp, exponential increase in the absolute value of the fractal head function.
2. The consolidation coefficient decreases from a value of $C_v \approx 0.6706$ at the initial point, to a value of $C_v \approx 0.4254$ at the final point. This decline in this case can be roughly approximated by the polynomials in Fig.1b.
3. Although considering all the simplifications, as well as the undoubted importance of the nature of the soil, which in the very first place determines the possible processes of both consolidation and fractal filtration; in general, we can say that homogeneous soil at given initial parameters and constants under the action of soil pressure will expand its fractal structure.
4. Although the graphs show unlimited growth, in real soil the process comes to naught rather quickly due to energy dissipation, heterogeneous layered structure and external particles in the soil, elasticity, elasticity and compressibility of both skeleton and fluid and a number of other factors.
5. Attempting to take into account all factors complicate drawing up and solving the problem. It seems much more reasonable to use empirical data with simplified models of soil behavior.
6. Rheological concepts are also important for the design of laboratory and field devices, in addition to standard test procedures. The solutions developed in the theory of consolidation of fluid-saturated reservoirs are relevant to the increasing amount of underground work in complex fields with high rock pressures, and to the design of processes for displacing hydrocarbon fluids from reservoirs.

## Acknowledgements

This research was funded by the SOCAR Scientific Foundation (Azerbaijan Republic) – project № 23 LR - AMEA.

## Nomenclature

$a_f$ – fluid compressibility;
$C$ – experimental coefficient;
$D_{\sigma'}$ – deviator of effective stress;
$e$ – porosity coefficient;
$i_0$ – head gradient.
$k_f$ – pore saturated fluid filtration coefficient;
$p_a$ – pressure in the soil pore;
$p_f$ – pressure in the pore saturated fluid;
$T_{\sigma'}$ – effective stress tensor;
$T_n$ – neutral stress tensor;
$T_p$ – post-action time;
$\alpha$ – fractality parameter of the filtration component;
$\gamma_f$ – fluid density;
$\xi$ – length of fractal element;
$\sigma_{m'}$ – average normal effective stress;
$\sigma_m$ – average linear stress;
$\sigma_z$ – stress of the soil skeleton;
$\sigma'(t)$ – time-varying effective pressure;

## References

[1] Markgraf W. (2011): *Rheology in soils. Encyclopedia of Agrophysics.*– Eds Glinski J., Horabik J. and Lipiec J., Springer Press, Dordrecht-Heidelberg-London-New York.
[2] Zhang J. and Tao G. (2011): *A new model for soil consolidation based on microstructure*.– J. Shanghai Jiaotong Univ., vol.16, No.1, pp.78-82, doi: 10.1007/s12204-011-1098-3.
[3] Fu X., Ding H., Sheng Q., Zhang Z., Yin D. and Chen F. (2022): *Fractal analysis of particle distribution and scale effect in a soil–rock mixture*.– Fractal Fract., vol.6, No.2, p.120, doi:10.3390/fractalfract6020120.
[4] Terzahgi C., Pek R.B. and Mesri G. (1996): *Soil Mechanics in Engineering Practice*.– John Willey and Sons, Inc., New York, p.534.
[5] Mashenko A.V., Ponomarev A.B. and Sychkina Y.N. (2014): *Special sections of soil mechanics and rock mechanics.*– Perm: Perm National Research Polytechnical University.
[6] Vyalov S.S. (1986): *Rheological Fundamentals of Soil Mechanics.*– Elsevier, Amsterdam, Netherlands, p.564.
[7] Mirzajanzadeh A.Kh. and Shakhverdiev A.Kh. (1997): *Dynamic processes in oil and gas production.*– Moscow: Nauka.
[8] Magara K. (1978): *Compaction and fluid migration: practical petroleum geology*.– Elsevier Scientific Pub. Co.
[9] Dobrynin V. (1970): *Deformations and variations of physical properties of oil and gas reservoirs*.– Moscow: Nedra.
[10] Iselidze O., Dakhnov A., Grigoryev Y., Semyonov E. and Kryukova I.B. (2018): *The effect of effective pressure on changes in the physical and reservoir properties of rocks.*– Gas Sci. Bull., vol.1, No.33, pp.95-99.
[11] Pachepsky Y., Crawford J.W. and Rawls W.J. (2000): *Fractals in soil science*.– Elsevier, vol.27, p295.
[12] Adler P.M., Thovert J.-F., Bekri S. and Yousefian F. (2002): *Real porous media: local geometry and transports*.– J. Eng. Mech., vol.128, No.8, pp.829–839, doi: 10.1061/(ASCE)0733-9399(2002)128:8(829).

[13] Balankin A.S. and Elizarraraz B.E. (2012): *Map of fluid flow in fractal porous medium into fractal continuum flow*.– Phys. Rev. E, vol.85, No.5, p.056314, doi: 10.1103/PhysRevE.85.056314.
[14] Huang B., Guo C., Tang Y., Guo J. and Cao L. (2019): *Experimental study on the permeability characteristic of fused quartz sand and mixed oil as a transparent soil*.– Water, vol.11, No.12, p.2514. doi:10.3390/w11122514.
[15] Sahimi M. (1993): *Flow phenomena in rocks: from continuum models to fractals, percolation, cellular automata, and simulated annealing*.– Rev. Mod. Phys., vol.65, No.4, pp.1393-1534, doi: 10.1103/RevModPhys.65.1393.
[16] Yu B. (2008): *Analysis of flow in fractal porous media*.– Appl. Mech. Rev., vol.61, No.5, doi: 10.1115/1.2955849.
[17] Nigmatullin R.R. (1992): *Fractional integral and its physical interpretation*.– Theor. Math. Phys., vol.90, No.3, pp.242-251, doi: 10.1007/BF01036529.
[18] Ivanov P. (1991): *Soils and foundations of hydraulic structures: soil mechanics*.– Moscow: "Vysshaya shkola".
[19] Golubev V.G. (2011): *Mathematical modeling of filtration in inhomogeneous fractured porous media*.– Bull. N.I. Lobachevsky Univ. Nizhny Novgorod, vol.4, No.3, pp.725-727.
[20] Panahov G.M. and Sultanov B.N. (2022): *Cyclic shock wave in soil and determination of changes in and displacements*.– Trans. ANAS, issue Mech., vol.42, no. 7, pp.44-52.
[21] Bohaienko V. and Bulavatsky V. (2020): *Fractional-fractal modeling of filtration-consolidation processes in saline saturated soils*.– Fractal Fract., vol.4, No.4, p.59, doi: 10.3390/fractalfract4040059.
[22] Bulavatsky V.M. (2021): *Closed solutions of some boundary-value problems of filtration-consolidation dynamics within the fractured-fractal approach*.– Cybern. Syst. Anal., vol.57, No.3, pp.383-395, doi: 10.1007/s10559-021-00363-9.

Received: October 10, 2022
Revised: January 30, 2023